Journal of Physiology (1995), **486.2**, *pp.*283–295

Imaging of calcium variations in living dendritic spines of cultured rat hippocampal neurons

Menahem Segal

Department of Neurobiology, The Weizmann Institute, Rehovot, 76100 Israel

1. Cultured rat hippocampal neurons were loaded with the Ca^{2+} indicator fura-2 through micropipettes and visualized with an inverted microscope equipped with a high power objective and a cooled CCD camera. The responses of dendritic spines and their parent dendrites to stimuli which evoke a rise of $[Ca^{2+}]_i$ were monitored.

2. NMDA caused a rapid and transient rise in $[Ca^{2+}]_i$, which was more evident in the spine than in the parent dendrite. The recovery in both compartments had the same time course, and was dependent on normal $[Na^+]_o$.

3. Application of α-latrotoxin, which causes release of neurotransmitters from terminals, produced a rise of $[Ca^{2+}]_i$ in the dendritic spines, more than in their parent dendrites. Prolonged exposure to the drug eliminated the spine/dendrite disparity.

4. The presence of voltage-gated calcium channels in dendritic spines is indicated by the enhanced calcium rise in spines rather than dendrites of cells depolarized by either intracellular current injection or by raising $[K^+]_o$. This rise was attenuated by nifedipine or verapamil, both L-type channel blockers.

5. It is suggested that the dendritic spine constitutes an independent calcium compartment that is closely linked to the parent dendrite.

Being the primary site of excitatory synaptic interaction in mammalian neurons, the dendritic spine has been proposed to play a pivotal role in neuronal plasticity (e.g. Malenka, Kauer, Perkel & Nicoll, 1989; Bliss & Collingridge, 1993). In trying to establish a role for the unique morphology of the dendritic spine, early theories proposed that the spine neck constituted a barrier/filter for synaptic currents (Rall, 1974; Koch & Poggio, 1983; Turner, 1984; Segev & Rall, 1988; Zador, Koch & Brown, 1990). In line with these hypotheses, some morphological changes have been detected in dendritic spines, correlating with neuronal activity (Lee, Schottler, Oliver & Lynch, 1980; Chang & Greenough, 1984; Muller, Gahwiler, Rietschin & Thompson, 1993). More recently, it has been proposed that the dendritic spine is a unique compartment, where the local concentration of a critical ion/molecule can rise to levels needed to activate cascades of chemical events associated with plasticity (Wickens, 1988; Koch & Zador, 1993). A prime candidate for such local effects is calcium. Calcium was found in dendritic spines (Fifkova, Markham & Delay, 1983), and flows into neurons following activation of the NMDA receptor (MacDermott, Mayer, Westbrook, Smith & Barker, 1986; Glaum, Scholz & Miller, 1990; Regehr & Tank, 1992; Wadman & Connor, 1992). Activation of ligand or voltage-gated calcium influx has been shown to constitute a necessary step in the process of long term synaptic modification in central neurons (Lynch, Larson, Kelso, Barrionuevo & Schottler, 1983; Malenka *et al.* 1989). It is therefore logical to assume that local changes in spine calcium concentration are crucial for plasticity. The small size of the spine, 0·2–1·0 μm, at the limit of optical resolution, has prohibited a systematic analysis of functional changes in this organelle using conventional electrophysiological approaches. However, the advent of new imaging techniques, along with the availability of sensitive detectors, now makes this analysis feasible. Preliminary studies, in the slice preparation, revealed that the spine can regulate calcium concentrations independently of the parent dendrite (Guthrie, Segal & Kater, 1991; Muller & Connor, 1991). However, the analysis of spine calcium concentration in the slice is hampered by the depth of the elements monitored in the tissue, and by the delicacy of the tissue, thus limiting the array of variables and time span for monitoring the spine. We have developed an *in vitro* dissociated tissue culture procedure (Segal & Manor, 1992) in which we can conveniently monitor calcium concentration changes in the individual spines and their parent dendrites of hippocampal neurons. While the tissue-cultured neuron is different in several respects from the neuron in the brain, it does grow dendritic spines which have all the morphological attributes of genuine dendritic spines (Papa, Bundman, Greenberger & Segal, 1995). We studied the effects of several stimuli on spine calcium ($[Ca^{2+}]_S$) and calcium in the adjacent dendrites ($[Ca^{2+}]_D$), and found that they are indeed dissociable.

METHODS

Cultures

Primary cultures of hippocampus were prepared from 19-day-old rat embryos as described previously (Segal & Manor, 1992). Briefly, pregnant Wistar rats were killed by rapid cervical dislocation, the embryos were removed and placed into sterile, ice-cold Leibovitz L15 medium, and immediately decapitated. The medium was oxygenated and enriched with 0·6% glucose and 15 μg ml^{-1} gentamycin. The hippocampus was dissected out, and the tissue was dissociated mechanically using a fire-polished Pasteur pipette in small volumes of L15. Tissue was suspended in plating medium consisting of 5% fetal calf serum and 5% heat-inactivated horse serum prepared in minimal essential medium (MEM) enriched with 0·6% glucose, 2 mM glutamine and 15 μg ml^{-1} gentamycin. Neurons were plated on 12 mm glass coverslips coated with 15 μg ml^{-1} poly-L-lysine, in a twenty-four-well plate, at a density of 500 000 cells per well. Three to four days after plating, the medium was changed to one containing 10% dialysed horse serum. With the first change of medium the cultures were treated with a mixture of uridine and 5-fluoro-2-deoxyuridine. The growth medium was changed once a week, if necessary.

Calcium measurements

Recordings were made from 2- to 5-week-old cultures. The coverslip was taken out of the well, washed in the recording medium and glued with silicon grease to the recording chamber. The chamber consisted of a plastic carrier with a well of 0·25 ml and a centre opening to hold the round coverslip. The chamber was placed on the stage of a Nikon inverted microscope, equipped with a UV light source, a computer-controlled filter wheel, and a fibre-optic light scrambler. Fluorescence signals following excitation of fura-2-filled cells with 340 and 380 nm wavelength light were collected on a Thompson 7883 288 × 384 pixel frame transfer chip installed in a Photometrics Cooled CCD camera (Photometrics, Tucson, AZ, USA). Images were stored on a Macintosh FX computer for off-line analysis. Calibrations of calcium concentrations were periodically made using standard solutions containing known concentrations of calcium ions (calcium calibration buffer kit, Molecular Probes), and the ratio of the fluorescence was measured with excitation at 340/380 nm, using the equation (Grynkiewicz, Poenie & Tsien, 1985):

$$[Ca^{2+}]_i = K_d F_{380}(R - R_{min})/(R_{max} - R),$$

where $[Ca^{2+}]_i$ is the intracellular calcium concentration, $K_d = 220$ nM (the fura-2–calcium dissociation constant), R_{min} and R_{max} are ratios of fluorescence to 340/380 nm excitations at minimal and maximal calcium concentrations, and F_{380} is the fluorescence emitted at 380 nm excitation, at limiting calcium concentrations. Curve fits to the estimated calcium values were better than $r = 0{\cdot}95$. The calculated values of $[Ca^{2+}]_i$ are tentative, at best, since the effects of the unique intracellular environment on properties of fura-2 are not very well known. Technical issues related to measurements of calcium in dendrites and spines are discussed below.

Procedures

Cells were first visualized with a ×40 phase objective lens. Individual, medium-large (15–25 μm in diameter) pyramidal and multipolar cells were impaled with sharp micropipettes containing 20 mM fura-2 at the tip and backfilled with 4 N potassium acetate. Membrane potential was monitored using an Axoclamp-2 amplifier. Input resistance was estimated from the response of the cell to constant 0·1 nA current pulses. The impaled cell was filled with fura-2 for 1–5 min using hyperpolarizing current pulses, and the magnitude of fluorescence was visualized at the fura-2 isosbestic wavelength (360 nm). Glass micropipettes, with tip diameters of 2–3 μm, were filled with glutamate (1 mM) α-latrotoxin (LTX, 3 nM), or *N*-methyl-D-aspartate (NMDA, 1 mM). Drugs were applied by 10–20 ms pressure pulses controlled by a digital stimulator (AMPI, Jerusalem) and synchronized with the acquisition of the images. In cases where a transient response to NMDA was sought (e.g. during a fast imaging sequence) a single 10–20 ms pulse was used. In cases where a high spatial resolution image was sought, requiring exposure to the fluorescent light for a total of 0·5–1 s, three to five pulses of NMDA were applied at a rate of 2 Hz. This caused a large and prolonged (up to 5–10 s) response to NMDA. Other drugs were applied through the perfusion medium. Following the loading of the cell with fura-2, the pipette was withdrawn (except when specified), and the cell viewed with a Fluor ×100 1·3 NA oil immersion Nikon lens. Regions of the dendrites containing apparent dendritic spines were then monitored. In some cases, the electrode microdrive was attached to the stage, allowing concurrent optical measurements at high resolution with recording of electrical signals from the cell dendrites and spines. A quick scan of the cells with both 340 and 380 nm wavelength light was used to select cells with a low resting $[Ca^{2+}]_i$ for analysis. Cells with high (> 100 nM) $[Ca^{2+}]_i$ were discarded. Routinely, two to three cells on a glass coverslip were injected with the dye, and the cells were visualized within 2 h of injection. To avoid photodynamic damage to the imaged cells, light was reduced using the iris diaphragm attached to the objective. The duration of the light exposure was varied as necessary, to obtain good spatial resolution.

Fast imaging

In the experiments involving fast imaging for measurements of time-dependent fluorescence changes, the field of view was reduced in size to the area of interest, including the spine(s) and adjacent dendrite (about 50 × 50 pixels), the pixels were binned into 2 pixel bins, and images of one wavelength (380 nm) were acquired at a rate of approximately one frame per 20 ms. An increase in $[Ca^{2+}]_i$ caused a reduction of fluorescence at this wavelength. For analysis, an area of interest in the middle of the spine (about 12–15 pixels) was compared with an equal area in the adjacent dendrite, or in the background. The fluorescence values (F) for all frames were normalized (F_n) and the change between the initial level of fluorescence (F_{min}) and the final level, in the presence of NMDA (F_{max}), was calculated (e.g. Fig. 2) such that:

$$F_n = 1 - (F - F_{min})/(F_{max} - F_{min}).$$

Solutions and drugs

The standard recording solution contained (mM): NaCl, 126; KCl, 4; $CaCl_2$, 2; $MgCl_2$, 1; Hepes, 10; and glucose, 4·2. pH was adjusted with NaOH to 7·4, and osmolarity adjusted to 320 mosmol (l solution)$^{-1}$ with sucrose. All experiments were conducted at room temperature. Tetrodotoxin (0·5 μM) was added to the recording solution before use. In some experiments involving responses to NMDA, $MgCl_2$ was omitted from the recording solution and 10 μM glycine was added. In Na^+-free medium, external Na^+ (Na^+_o) was replaced by *N*-methyl-D-glucamine (NMG). Drugs were purchased from Molecular Probes (USA), Sigma and Tocris Neuramin (Bristol, UK). α-Latrotoxin (LTX), purified from black widow spider (*Latrodectus fredecemgutattus*), ω-conotoxin GVIA (ω-conotoxin), and ω-agatoxin-IVA (agatoxin) were gifts from Alomone Labs (Jerusalem).

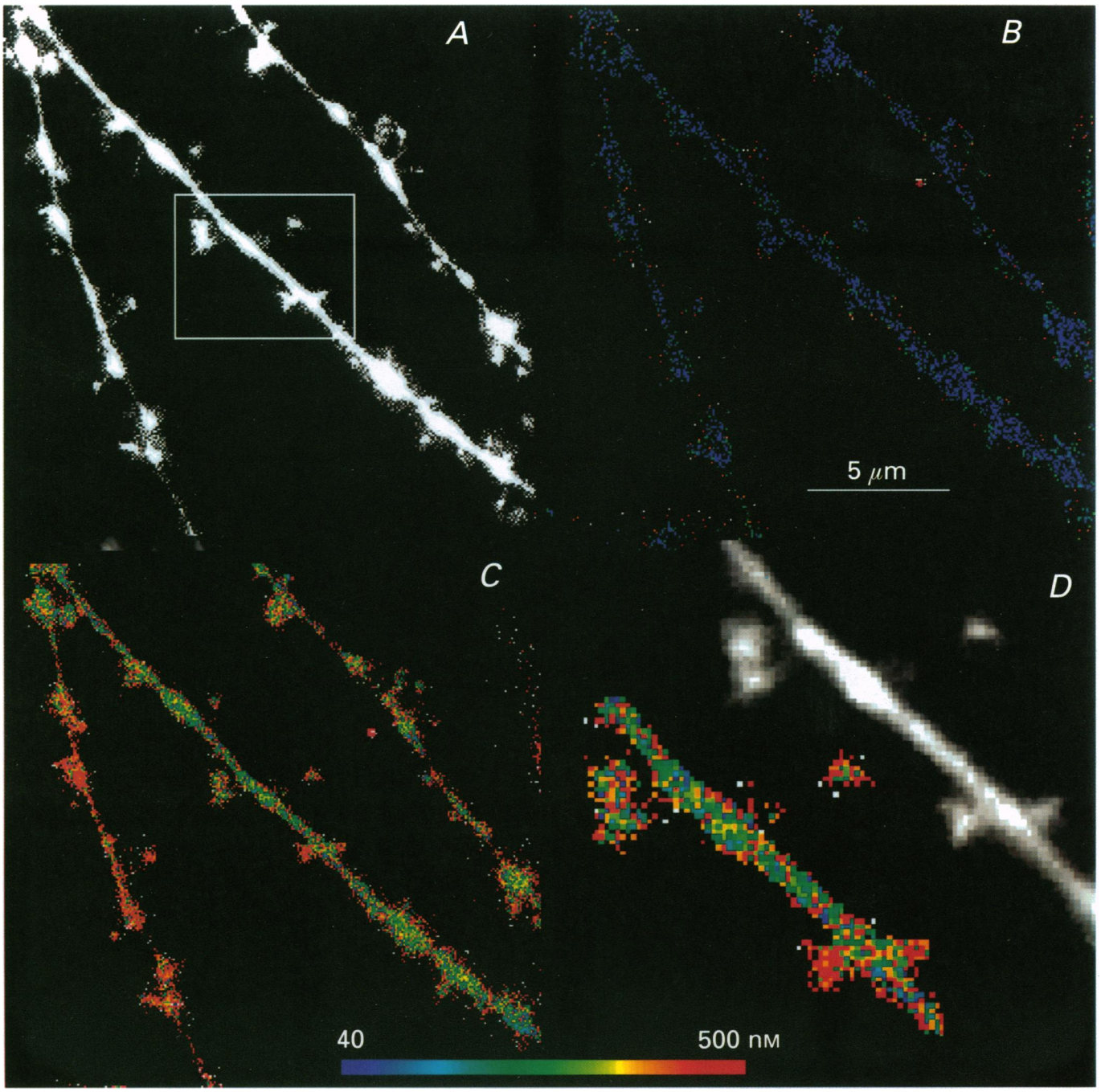

Figure 1. NMDA evokes a rise of $[Ca^{2+}]_i$ in spines and adjacent dendrites

Computer-generated, pseudocolour images of calculated calcium concentrations before and after topical application of NMDA. *A*, raw image taken at the isosbestic wavelength (360 nm) of dendrites and spines of a single neuron at rest. *B*, pseudocolour image of the same dendrites at rest, indicating a low and similar level of $[Ca^{2+}]_i$ in all (but one) spines and dendrites. *C*, during response to NMDA, images taken within 0·5 s of application of three pulses of the drug at rapid rate. Images were taken with the slow acquisition rate, 0·5 s per frame, for the 340 and 380 nm illumination. It illustrates a differential response of spines and dendrite to the drug. Note that the dendrite on the left has higher values of $[Ca^{2+}]_i$ than the centre and right dendrites. *D*, high-power images of a section of the dendrite seen in *A*. Note the difference in calcium changes among adjacent spines. Scale, 5 μm; colour scale, 40–500 nM $[Ca^{2+}]_i$.

Analysis

Measurements were made from apparent dendritic spines, identified as short, 0·5–2 μm extrusions from, and usually at right angle to, dendrites. These were clearly distinguished from short or out-of-focus dendrites in that their end tip was clearly visualized. Larger spines were preferred to shorter ones, even if they were larger than 2 μm, since they allowed a clearer separation between spines and dendrites. Special care was taken to measure calcium levels at the core of the spine in an isolated segment with no other neuronal element in the light path, above or below the spine. The area measured was a rectangle of up to 8 × 8 pixels, and not smaller than a total of 12 pixels. At the magnification used, a micrometer length was enclosed in 8·5 pixels. Measurements were also made from the adjacent, naked parent dendrite, as close as possible to the measured spine. Care was taken to avoid measurements of regions of dendrites containing out-of-focus spines. Data were only analysed from spines and their parent dendrites that were in sharp focus throughout the experiment. Comparisons of $[Ca^{2+}]_i$ were always made between spines (S) and their adjacent dendrites (D), and are expressed as the ratio S/D. This helped to reduce variability caused by inhomogeneity among nearby spines and among different regions of the same dendrites. While not all spines expressed higher $[Ca^{2+}]_i$ values than their parent dendrites, for analysis purposes all S/Ds in a given

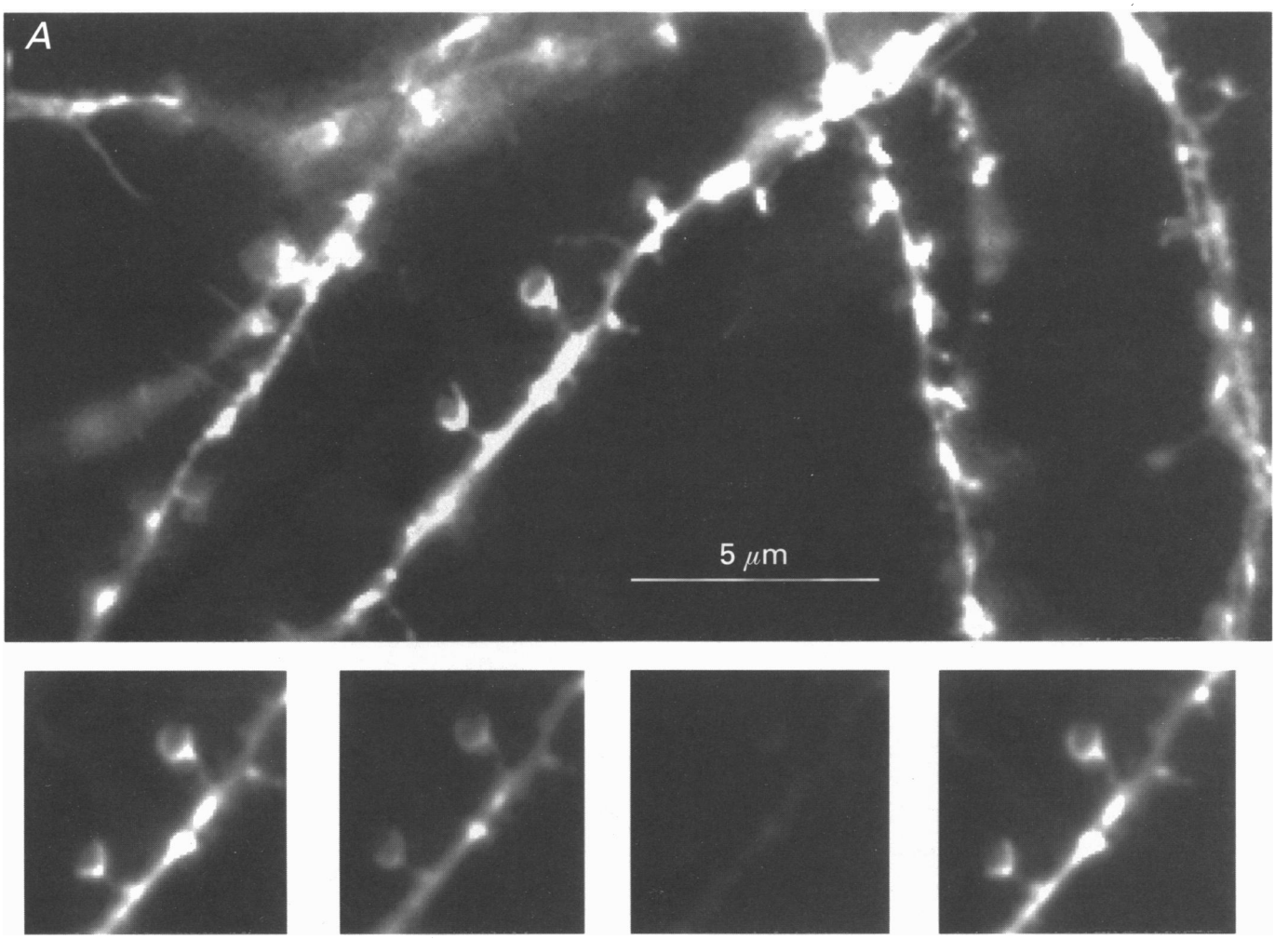

Figure 2. Time course of change in fluorescence to excitation at 380 nm, during the response to NMDA

Frames were taken at 20 ms intervals. *A*, an image of dendrites and spines taken at 360 nm, from which a region in the centre was selected for fast imaging. Bottom, four successive images were taken, from left to right, at 380 nm during exposure to NMDA, and after recovery, right. *B*, a single experiment measuring $[Ca^{2+}]_i$ in one spine and its adjacent dendrite at resting conditions (spon, spontaneous) and during the response to NMDA. Note the fluctuation of the response to NMDA in the spine and not in the parent dendrite during the rise of $[Ca^{2+}]_i$. Ordinate scale is normalized fluorescence change, as detailed in the text. *C*, mean responses to NMDA in 9 spine–dendrite pairs. The rise of $[Ca^{2+}]_i$ following application of the drug is shown on an expanded time scale. Application of NMDA is indicated by the arrow. The three baseline points prior to application of NMDA are means of 5–6 measurements each, the rest are means of 9 spine–dendrite pairs. A clear difference between the mean rise in spines and the dendrites in rate of rise of $[Ca^{2+}]_i$ is seen already at the tenth 20 ms time point.

experiment were used for the mean S/D ratio (i.e. there was no selection of the data based on the size of the individual S/D ratio) and the results were subjected to Student's paired t tests, when applicable. Subtraction of background was made from regions of the image remote from the spine. There were no fluorescence signals outside the filled neurons and the signal-to-noise ratio was high, even in the fast imaging series.

One to two fields were imaged in each cell. Viability of the spines/dendrites was verified by the complete recovery to resting calcium levels after an evoked calcium rise, whenever possible. Several successive applications of NMDA or glutamate resulted in a similar transient rise of $[Ca^{2+}]_i$. Paired spine–dendrite samples were compared by Student's paired t tests.

RESULTS

Resting calcium levels

Recordings were made from medium-sized (15–25 μm) pyramidal and multipolar cells. The recorded cells could be divided into aspiny, sparsely spiny and spiny cells. The former group had long, relatively unbranched, thin dendrites, and were shown in previous studies to be immunopositive for GAD, the enzyme marker for GABA (Segal & Greenberger, 1992). The sparsely spiny cells had less than one spine per 10 μm dendritic segment. The spiny cells had a high density of spines, approaching three to five spines in a 10 μm segment (Fig. 1). Spines varied in length (from 0·5 to over 2 μm), and in shape (from simple extrusions from the dendrite, to mushroom-shaped spine heads of over 0·5 μm, and necks of less than 0·2 μm in diameter). Calcium measurements were made from these mushroom-shaped spines, on secondary and tertiary dendrites. Further details of the spine morphology are presented elsewhere (Papa *et al.* 1995).

$[Ca^{2+}]_i$ was measured in over 400 dendritic spines and adjacent dendrites from over 120 cells. Estimated resting values of $[Ca^{2+}]_i$ in a random sample of 35 spines and their adjacent dendrites were 45·3 ± 3·6 and 41·8 ± 3·5 nM (means ± S.E.M.), respectively, yielding a mean S/D ratio (the ratio of $[Ca^{2+}]_i$ in the spine over $[Ca^{2+}]_i$ in the dendrite) of near 1·0. There was no apparent correlation between resting $[Ca^{2+}]_i$ or S/D ratios among the different spine shapes or sizes.

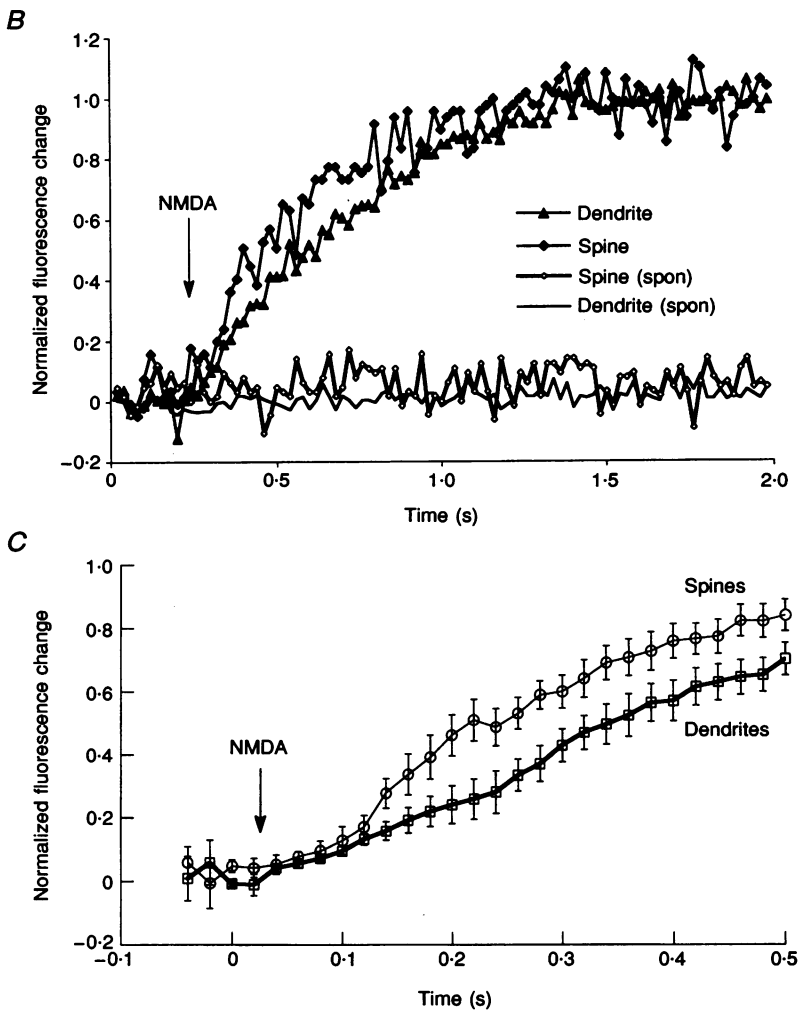

Figure 2*B* and *C*. For legend see facing page.

Table 1. Summary of calcium changes in spines and dendrites

Expt	Treatment	$[Ca^{2+}]_S$ (nM)	$[Ca^{2+}]_D$ (nM)	S/D	n (pairs)
1	NMDA	331	250	1·40	31
2	LTX	204	159	1·37	24
3	Long LTX	476	499	0·97	15
4	LTX (II)	301	270	1·11	17
5	Voltage (−20 mV)	193	153	1·26	14
	Voltage (0 mV)	277	253	1·09	14
6	High K^+	291	244	1·21	34
7	Long high K^+	465	472	0·98	12
8	High K^+ (−Ver)	455	419	1·09	22
	High K^+ (+Ver)	167	152	1·10	22

Expt, experiment number. Expt 5 is the same group of spines tested in two voltage conditions. Expt 8, the same spines tested in control and in the presence of veratridine (Ver). Results are means of $[Ca^{2+}]_i$ (nM). n denotes the number of spine–dendrite pairs. Further details are in the text.

Responses to NMDA

Pressure application of NMDA resulted in a rapid, large and transient rise of $[Ca^{2+}]_i$ in both spines and parent dendrites (Fig. 1). The evoked $[Ca^{2+}]_i$ in spines was 331 ± 38 nM ($n = 31$). The rise in the parent dendrites was 250 ± 28 nM, and the mean S/D ratio was $1{\cdot}40 \pm 0{\cdot}07$ (Student's t value, 4·68, $P < 0{\cdot}001$, Table 1). The responses to NMDA were different among adjacent spines on a single dendrite, but were more similar than spines on different dendrites in a given field of view (Fig. 1). In general, there were no 'hot spots' on dendrites that were restricted in size akin to the changes seen in the spines. There were some differences between dendrites in reactivity to NMDA, but these usually involved large sections of the dendrites. Of the thirty-one spines measured in this sample, twenty-four exhibited a higher $[Ca^{2+}]_i$ response compared with their parent dendrites, producing a S/D ratio of at least 1·1 whereas the other seven spines were not different from their parent dendrites. Some of these differences may be associated with the shape of the spine, in that mushroom-shaped spine heads with long necks appeared to have higher S/D ratios than smaller spines, but there were

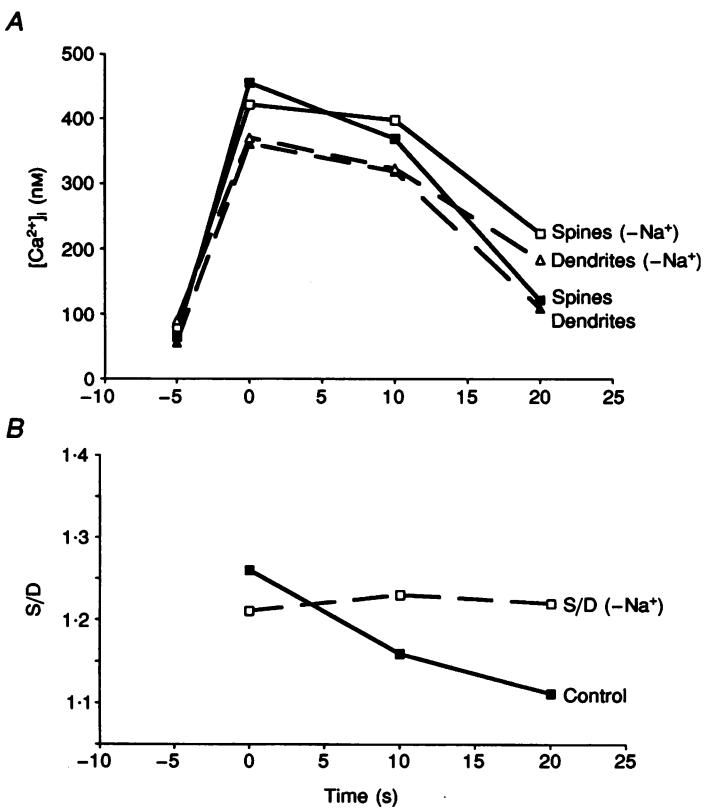

Figure 3. The recovery from the effects of NMDA depends on normal $[Na^+]_o$

A summary of changes in $[Ca^{2+}]_S$ and $[Ca^{2+}]_D$ following application of NMDA in the presence and absence ($-Na^+$) of sodium in the bathing medium. NMDA caused a rise in $[Ca^{2+}]_i$ to about 400 nM (*A*). The S/D ratio went up to 1·26. Intracellular calcium concentration came back close to control level within 20 s under control conditions. The S/D ratio also came back to about 1·1 within this time course (*B*). In the absence of $[Na^+]_o$, the recovery of $[Ca^{2+}]_i$ was slower, and the S/D ratio remained elevated. $n = 13$ spines in 5 experiments.

exceptions to this rule, and no systematic differences among spine shapes and size of calcium responses were seen. The response to NMDA depended on the activation of an NMDA receptor, as it was blocked by 25 μM 2-amino-5-phosphonovaleric acid (2-APV) (3 experiments, data not shown). Likewise, the response was dependent on the presence of normal $[Ca^{2+}]_o$; in the nominally calcium-free medium, NMDA was ineffective (4 experiments, 12 spines). Voltage-gated calcium channels do not seem to contribute much to the calcium responses to NMDA; blockade of the L-type channel with 20 μM nifedipine did not change the responses to NMDA, as seen previously (Segal & Manor, 1992) (3 experiments).

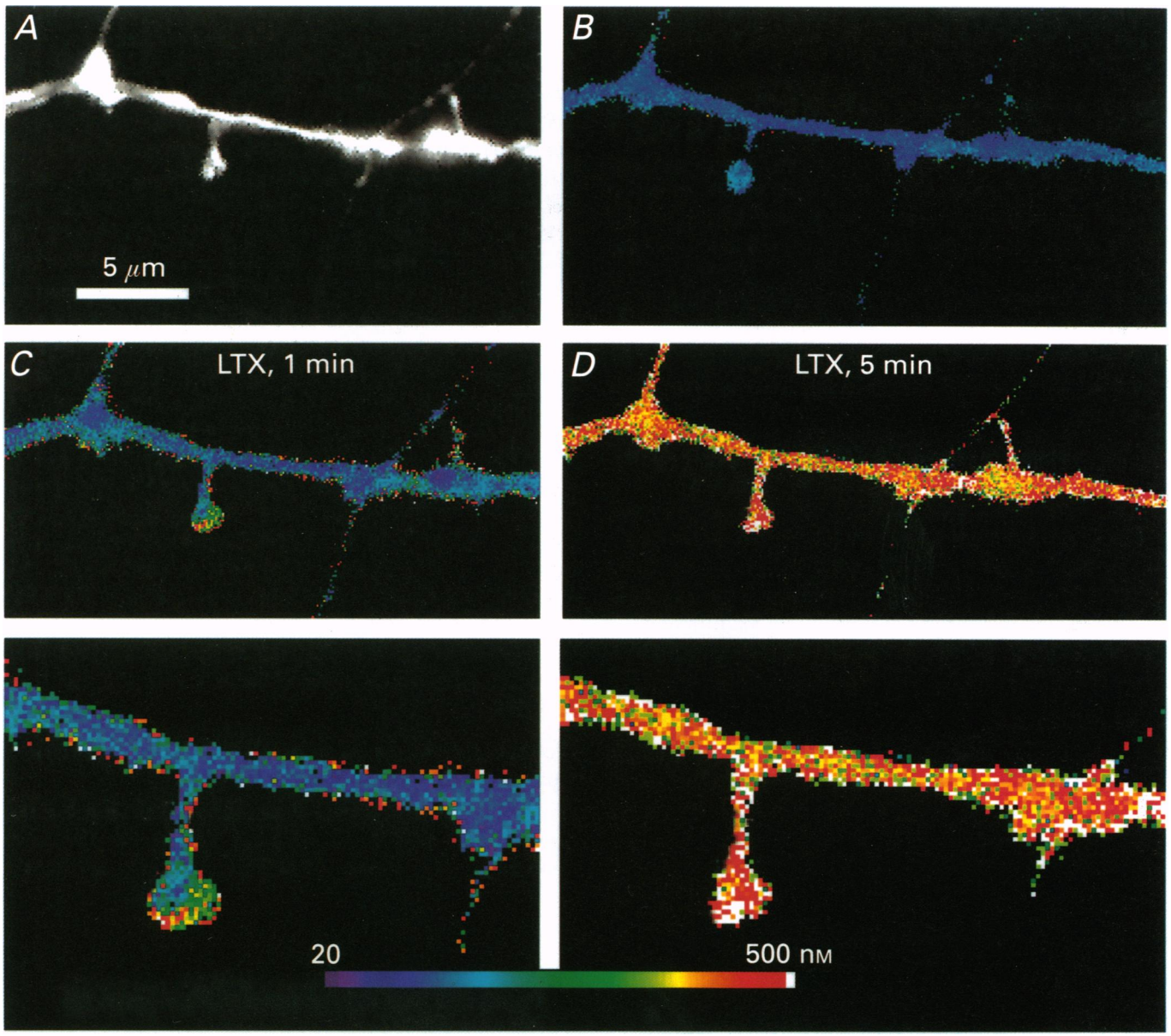

Figure 4. LTX reduces a rise of $[Ca^{2+}]_s$

Pseudocolour images of calculated calcium concentrations in a dendritic segment. *A*, an image of the dendrite and spines illuminated at 360 nm. A small spine is seen on the right, in close approximation to a passing fibre originating in an adjacent, stained neuron. *B*, resting level of $[Ca^{2+}]_i$ in the dendrite and the spines. *C*, 1 min after onset of exposure to LTX, a rise of $[Ca^{2+}]_s$ is clearly higher in the two spines seen than in the dendrite. *D*, when calcium rises throughout the dendrite, 5 min following application of LTX, there is a smaller difference between spines and the dendrite. Bottom, corresponding high power images of those seen in *C* and *D*. Note the gradient of calcium rise in the spine.

The rise time of elevated $[Ca^{2+}]_i$ following a single 20 ms pulse application of NMDA was assessed using fast acquisition of single wavelength (380 nm) small frame images (Fig. 2). The rise of $[Ca^{2+}]_S$ preceded that of $[Ca^{2+}]_D$ in all cases examined ($n = 9$ spines). The rise in $[Ca^{2+}]_S$ reached half-maximum on average about 220 ms after the application of NMDA, whereas a similar rise was seen in the adjacent dendrite within 340 ms (Fig. 2*B*). The pattern of rise was different in the two compartments: the change in $[Ca^{2+}]_D$ was gradual and smooth, whereas the change in $[Ca^{2+}]_S$ fluctuated more (Fig. 2*B*).

The time course of recovery from the NMDA-evoked rise of $[Ca^{2+}]_i$ was measured by taking successive high spatial resolution ratio images after drug application (Fig. 3). NMDA was applied in three successive pulses to reach plateau values. It caused a rise of both $[Ca^{2+}]_S$ and $[Ca^{2+}]_D$, with a higher rise in the former compartment ($t = 2{\cdot}44$, $P < 0{\cdot}015$). Within 20 s of the peak of the evoked rise in $[Ca^{2+}]_i$ there was a near-complete recovery of $[Ca^{2+}]_i$ to resting levels. Within this time interval the $[Ca^{2+}]_S$ recovered to a level similar to that of $[Ca^{2+}]_D$ (Fig. 3). Sustained levels of $[Ca^{2+}]_i$ were rarely seen in the spines examined.

The involvement of a sodium–calcium exchanger in the recovery from the effects of NMDA was assessed using a low Na^+-containing medium (Fig. 3). Absence of Na^+ slowed down the rate of recovery following the calcium load (comparing control with $0\,[Na^+]_o$ conditions at 20 s, $t = 3{\cdot}71$, $P < 0{\cdot}0009$) In addition, the S/D ratio remained elevated during recovery from the calcium load, indicating that the sodium–calcium exchanger serves an important role in the fast recovery of the spine from excess calcium.

Effects of α-LTX

The present experiments do not rule out the possibility that the calcium rise seen in the parent dendrite actually results from activation of both synaptic and extra synaptic NMDA receptors located on the dendritic shaft, and not from the spread of calcium from the spine into the dendrite. To activate synaptic receptors directly we used the potent neurotransmitter releaser α-latrotoxin (LTX; Grasso, Alema, Ruffini & Senni, 1980). LTX (0·5 nM in the bath or 3 nM in a pressure pipette) caused, within 5 min of the drug application, a rise in both $[Ca^{2+}]_S$ and $[Ca^{2+}]_D$, to 204 ± 19 and 159 ± 18 nM, respectively (Fig. 4). The S/D ratio was $1{\cdot}37 \pm 0{\cdot}10$ ($t = 4{\cdot}60$, $n = 24$, $P < 0{\cdot}001$, Table 1). Not all the spines were higher than their parent dendrites in the $[Ca^{2+}]_i$ response during exposure to LTX. In only sixteen of the twenty-four S–D pairs was this difference seen (i.e. the S/D ratio was larger than 1·1, see above) whereas the other eight spines had a similar $[Ca^{2+}]_i$ response to their parent dendrites. Exposure to the drug for longer periods of time, or to higher concentrations of the drug (2–5 nM), resulted in a large and irreversible increase of $[Ca^{2+}]_S$ to 476 ± 27 nM and $[Ca^{2+}]_D$ to 499 ± 33 nM, with a non-significant S/D ratio of $0{\cdot}97 \pm 0{\cdot}03$ ($n = 15$, Table 1). In another series of experiments, the possibility that the effects of LTX are due to release of excitatory neurotransmitters from presynaptic terminals or to a direct action of the drug on the recorded cells, was examined. In the presence of 50 μM 2-APV, LTX failed to elicit a rise in $[Ca^{2+}]_i$ (5 experiments, 17 spines measured); in control conditions LTX caused, within 5 min of its application, a rise of $[Ca^{2+}]_S$ and $[Ca^{2+}]_D$ to 301 ± 29 and 270 ± 19 nM, respectively, whereas in the presence of 2-APV, $[Ca^{2+}]_S$ and $[Ca^{2+}]_D$ went up, within 5 min of drug application, to 77 ± 14 and 82 ± 18 nM, respectively. Following washout of 2-APV, $[Ca^{2+}]_S$ and $[Ca^{2+}]_D$ went up to levels seen in the control, LTX-treated cells. This blocking action of 2-APV was seen only with a moderate dose of LTX; higher concentrations of the drug (2–5 nM in the perfusion medium, 2 experiments) did cause an elevation of $[Ca^{2+}]_i$ in the presence of 2-APV.

Voltage-gated calcium channels(VGCCs) in dendritic spines

Two types of experiments were conducted to examine the presence of VGCCs in dendritic spines. In the first, recordings were taken intracellularly while measuring

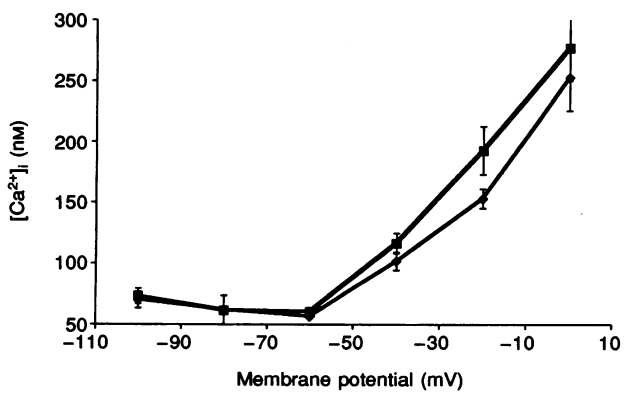

Figure 5. Voltage dependence of $[Ca^{2+}]_i$ in spines (■) and dendrites (◆)

Cells were recorded with micropipettes containing fura-2 and potassium acetate, and current clamped to various potentials, negative and positive to the resting potential. A significant rise in $[Ca^{2+}]_i$ was seen when the cells were held at or positive to −20 mV. At −20 mV there was a significantly higher rise of $[Ca^{2+}]_i$ in the spines than the dendrites ($n = 14$ spine–dendrite pairs).

calcium concentration in dendrites and spines. In these cases, the microelectrode manipulator was attached to the stage of the microscope, and recording of membrane potential was made while the cell was visualized at high power. In ten cells (14 spine–dendrite segments) examined, resting membrane potential was about −60 mV and input resistance in excess of 80 MΩ. Depolarization or hyperpolarization was accomplished by passage of constant current through the recording electrode. Resting levels of calcium in the dendrites were not different from those in the spines at membrane potentials less than −30 mV. However, depolarization of the cells to −20 mV resulted in a larger rise of $[Ca^{2+}]_S$ compared with that of the $[Ca^{2+}]_D$ (Fig. 5). This difference was statistically significant (S/D ratio = 1·26, $t = 2·0$, $n = 14$, $P < 0·05$). Further depolarization to 0 mV resulted in an additional increase in the $[Ca^{2+}]_i$ of both spines and dendrites but there was no difference in the mean values of the two compartments (S/D ratio = 1·09, $P > 0·05$, Fig. 5).

In the second, cells were depolarized by perfusing them with a high K^+-containing medium. In some experiments, 90 mM Na^+ was replaced by 90 mM K^+, to maintain an isosmotic medium. In addition, the medium contained 20 μM 2-APV, to prevent activation of NMDA receptors by released glutamate. Rapid perfusion with 90 mM K^+ produced, within 10 s of exposure, a rise of $[Ca^{2+}]_S$ from 34·7 ± 2·6 to 291 ± 13·9 nM and $[Ca^{2+}]_D$ from 35·8 ± 3·7 to 244 ± 12·6 nM, and a significant S/D ratio of 1·21 ± 0·03 ($n = 34$, Fig. 6). In another series of experiments, a prolonged (5 min) exposure of the cells to 90 mM K^+ yielded similar elevations of $[Ca^{2+}]_S$ and $[Ca^{2+}]_D$, to 465 ± 22 and 472 ± 19 nM, respectively, with a S/D ratio of 0·98 (12 S–D segments).

The type(s) of VGCC underlying the depolarization-induced rise of $[Ca^{2+}]_i$ were studied using calcium channel blockers. In the presence of 10–20 μM nifedipine, 90 mM K^+ caused a rise of $[Ca^{2+}]_S$ to only 119·7 ± 18·9 nM and $[Ca^{2+}]_D$ to 110·5 ± 16·0 nM, and a non-significant S/D ratio of 1·07 ± 0·04 ($n = 25$ spines). In another series of four experiments, cells were examined in the absence and presence of 40 μM verapamil. The high K^+-containing medium raised $[Ca^{2+}]_S$ to 455 ± 26 nM and $[Ca^{2+}]_D$ to 419 ± 22 nM ($n = 22$ spine–dendrite segments, S/D ratio of 1·09 ± 0·02). In the presence of verapamil the high K^+-containing medium caused a rise of $[Ca^{2+}]_S$ and $[Ca^{2+}]_D$ to only 167 ± 10 and 152 ± 9·7 nM, respectively. This constitutes a reduction of about 70% in the K^+-evoked rise of $[Ca^{2+}]_i$.

The type of VGCC associated with the increase in $[Ca^{2+}]_i$, which is not related to L-type channels (i.e. not blocked by nifedipine and verapamil), was studied using agatoxin (at 200 nM, a blocker of P-type calcium channels (Mintz, Adams & Bean, 1992)) or ω-conotoxin (at 2 μM, a blocker of N-type calcium channels (Aosaki & Kasai, 1989)). Both drugs were applied by perfusion, before and during

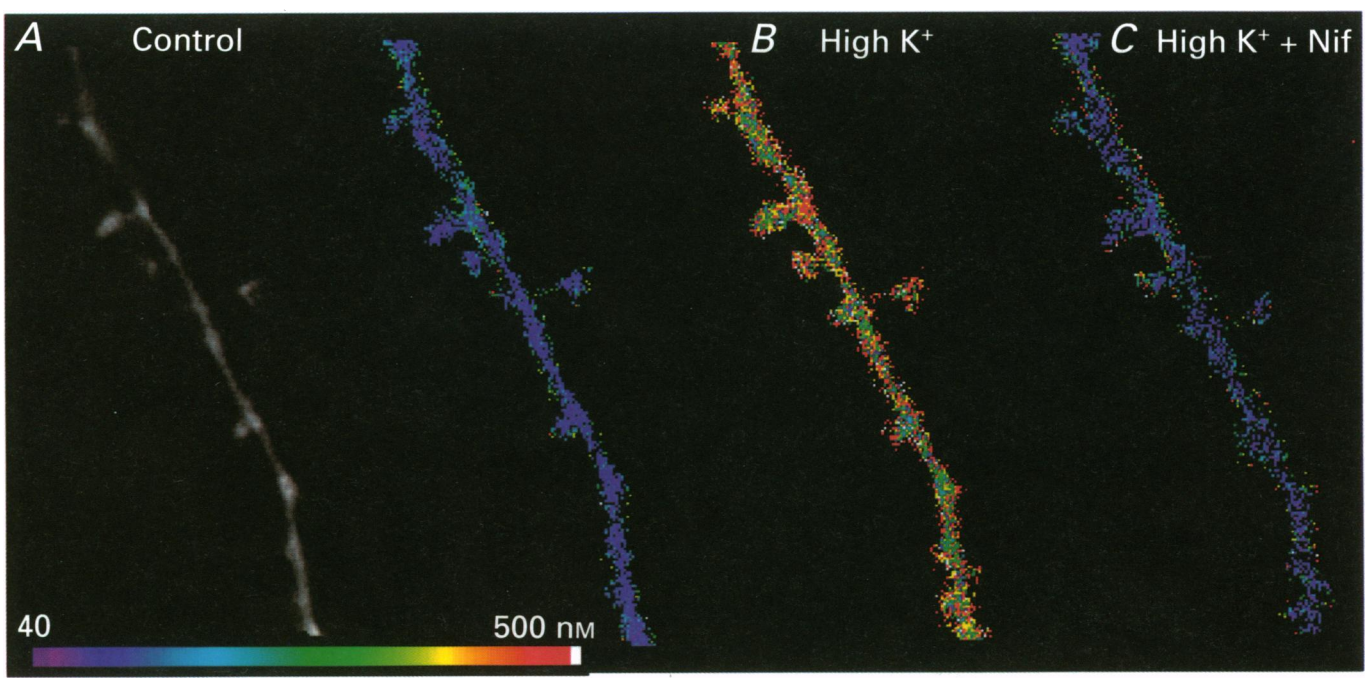

Figure 6. Depolarization induces a rise of $[Ca^{2+}]_i$ in dendrites and spines

The culture was exposed to 90 mM KCl, replacing NaCl. *A*, from left to right, raw image, ratio image at rest. *B*, image during exposure to 90 mM K^+. *C*, image during exposure to 90 mM K^+, in the presence of 10 μM nifedipine (Nif).

exposure to a high K^+-containing medium. In five experiments, ω-conotoxin failed to reduce the $[Ca^{2+}]_i$ responses of dendrites to a high K^+-containing medium which was 435 ± 64 nM in control conditions, and 485 ± 109 nM in the presence of antagonist. Likewise, agatoxin did not change dendritic responses to high K^+-containing medium, which was 487 ± 73 nM in control conditions and 488 ± 85 nM in the presence of the drug (6 experiments). No specific S/D measurements were made in these experiments, but they indicate that neither N- nor P-type channels contribute much to the $[Ca^{2+}]_i$ rise caused by depolarization of these dendrites.

DISCUSSION

The present results demonstrate that cultured hippocampal neurons can raise $[Ca^{2+}]_i$ in their dendrites and spines in response to topical application of neurotransmitter substances, synaptic stimulation, and activation of VGCCs. In these conditions, $[Ca^{2+}]_S$ rose to a level higher than that reached in the adjacent parent dendrites ($[Ca^{2+}]_D$) by up to an average of 40%. Following the rise in $[Ca^{2+}]_i$, a recovery to predrug levels could be reached within 10–30 s, in both spines and dendrites. Whenever a recovery was not seen (e.g. as with prolonged exposure to high K^+ or LTX), the rise of $[Ca^{2+}]_D$ reached the level of the rise of $[Ca^{2+}]_S$. The presence of voltage-gated calcium channels in the dendritic spines is indicated by the calcium response to depolarization, evoked either by passage of constant current across the membrane or by high $[K^+]_o$, resulting in S/D ratios significantly greater than 1. This response was blocked by calcium channel antagonists nifedipine and verapamil.

The fact that $[Ca^{2+}]_S$ increased more than $[Ca^{2+}]_D$ in response to stimulation may reflect one of several features of the spine. It is likely that the spine contains a higher concentration of NMDA receptors and VGCCs and/or lower concentrations of calcium-handling mechanisms than the parent dendrite. It is also possible that the unique morphology of the spine relative to the dendrite, i.e. the spine being a sealed-end organelle, with a limited volume to buffer calcium, compared with the large, open-ended structure of the dendrite, determines its unique properties. Finally, it is possible that the values of $[Ca^{2+}]_i$ in the spines reflect some kind of a systematic artifact of measurement.

This latter possibility is least likely because the spines selected for analysis were clearly distinguished from surrounding tissue, and the calcium fluorescence signal in the spines was much higher than the background noise. If anything, the fluorescence signal in the dendrites may have been contaminated by calcium measurements in out-of-plane spines, which will act to reduce the S/D difference. Whenever the spines and dendrites were clearly isolated, the concentration of the dye, estimated by the fluorescence to the isosbestic wavelength of 360 nm, was similar in the two compartments.

The unique structure of the spine, being a small, sealed-end structure, cannot explain all the observed S/D difference. Obviously, not all spines expressed a higher calcium change compared with their parent dendrites, and there was no clear correlation between S/D ratio and shape of the spine. In only about 2/3 of the spines were these differences large and consistent. The reason why not all spines express a larger calcium response is not clear, but it may be to do with the innervation pattern of the spines or the distribution of receptors on them.

The observed S/D ratio could be caused by an inhomogeneous distribution of NMDA receptors on dendrites and spines. It is, in fact, expected that if most of the excitatory terminals on pyramidal cells synapse on spines, then spine-associated receptors will cause a preferential rise of $[Ca^{2+}]_i$ in spines. A recent immunohistochemical study of the distribution of glutamate receptors found a proportion of these receptors on both dendritic shafts and spines of cultured hippocampal neurons (Craig, Blackstone, Huganir & Banker, 1993). We were able to replicate these observations, and found a patchy distribution of NMDA receptors, which were by no means restricted to dendritic spines (M. Segal, M. Papa & V. Greenberger, unpublished observations). Likewise, patchy distribution of clusters of NMDA receptors were found on dendrites of live cells in culture, and these too were not restricted to dendritic spines (Benke, Jones, Collingridge & Angelides, 1993). Also, synaptophysine-immunoreactive terminals were found on both dendritic spines and dendritic shafts (Papa *et al.* 1995), indicating that a preferential localization of NMDA receptors on spines is not likely to be the sole explanation of the S/D ratios found here.

The diameter of the dendrite relative to that of the spine is probably also not the sole factor in this respect, as some of the measurements taken in the present study are from small-diameter dendrites having large spine heads. These cases, illustrated in Figs 1 and 2, produced large S/D ratios. Altogether, the relative diameters of the spines and dendrites were not correlated with the S/D calcium ratios. Also, the distance between the spine head and the dendritic shaft was not clearly correlated with the S/D ratio as relatively remote spines did not have a clearly higher $[Ca^{2+}]_i$ than nearby spines (e.g. Fig. 1). It is likely that both the preferential localization of receptors and channels, and the unique, sealed-end structure of the spine contribute to the higher $[Ca^{2+}]_S$ than $[Ca^{2+}]_D$. Interestingly, in both LTX, and the high K^+-induced rise of $[Ca^{2+}]_i$, a prolonged exposure of the cell to these agents eliminated S/D difference. This was typically associated with a large

$[Ca^{2+}]_i$ rise, and may indicate breakdown of calcium removal mechanisms and S/D differentiation. Whatever it indicates, the elimination of the S/D ratio in some conditions adds credibility to the presence of such a significant ratio during the responses to synaptic and chemical stimulation.

The relatively low rise of $[Ca^{2+}]_i$, in the range of 0·3–0·5 μM, and the slow time course of the effects of NMDA on $[Ca^{2+}]_i$ are probably due to the high buffering capacity of these neurons caused by the addition of fura-2 to the cell. The recording pipette contained 20 mM of fura-2 at the tip, which resulted in a concentration of about 0·5 mM of the dye in the recorded cell. This estimate is based on some experiments in which the cell was recorded with a patch pipette containing 0·1–1·0 mM fura-2, where the concentration of the dye in the cell equilibrates with that of the pipette. This concentration of the dye was needed in order to obtain a good quality spatial resolution of the spines, but it most probably affected the calcium response properties of the dendrites and spines, as seen elsewhere (Regher & Tank, 1992). Thus, these estimates of $[Ca^{2+}]_S$ and $[Ca^{2+}]_D$ are conservative, but should not affect S/D ratios much.

While the time course of recovery from the effect of NMDA appears to be rather slow, following a large increase in $[Ca^{2+}]_i$, it was similar in the spine and the dendrite. Rarely was sustained and selective elevation of $[Ca^{2+}]_i$ found in individual spines. This may reflect a difference between cells in slices (Muller & Connor, 1991) and culture (see also Murphy, Baraban, Wier & Blatter, 1994), although other studies in slices with a confocal laser scanning microscope imaging and synaptic stimulation also failed to detect sustained changes in $[Ca^{2+}]_S$ (Alford, Frenguelli, Schofield & Collingridge, 1993; Jaffe, Fisher & Brown, 1994).

The existence of voltage-gated calcium channels on dendritic spines is indicated by the larger rise of $[Ca^{2+}]_S$ than $[Ca^{2+}]_D$ in response to depolarization. This difference was seen both when the cells were depolarized with intracellular current injection or with rapid perfusion with high K^+-containing medium. A similar suggestion for the presence of VGCCs on dendritic spines was reported recently (Jaffe *et al.* 1994). The presence of VGCCs on dendritic spines has important implications for the integrative capacity of individual dendritic spines, as alluded to elsewhere (Wickens, 1988; Jaffe *et al.* 1994).

The type of VGCC underlying the depolarization-induced rise in $[Ca^{2+}]_i$ has been studied using the L-type channel blockers nifedipine and verapamil, which markedly reduced the $[Ca^{2+}]_i$ rise. L-type channels have been localized on somata and proximal dendrites but less on distal dendrites of hippocampal neurons *in vivo* (Hell *et al.* 1993). While a careful comparison between the spatial distribution of L-type channels between cultured and *in vivo* neurons has not been made, a deviation in regulation of expression of these channels in the cultured neurons cannot be ruled out.

The relative contribution of VGCCs and NMDA channels to the rise of spine calcium concentration is not clear; both of these can raise $[Ca^{2+}]_i$, and NMDA can do this in voltage-clamped cells (MacDermott *et al.* 1986). There is a debate as to which is the primary mediator of the synaptically activated rise of dendritic calcium, the NMDA-related channels (Regher & Tank, 1992; Collingridge, 1992; Alford *et al.* 1993; Malinow, Otmakhov, Blum & Lisman, 1994) or VGCCs (Miyakawa *et al.* 1992; Markram & Sakmann, 1994). Our ability to reduce or delay the rise of $[Ca^{2+}]_i$ produced by LTX with the NMDA antagonist 2-APV indicates that NMDA channels play an important role in raising $[Ca^{2+}]_i$ subsequent to synaptic stimulation in our test system. The accurate determination of both contributions will require voltage clamp analysis of the synaptic responses simultaneously with the calcium measurements.

Being a focus of attention in central synaptic communication, a number of groups have recently begun to study calcium changes in the dendritic spine (Alford *et al.* 1993; Pozzo Miller, Petrozzino, Mahanty & Connor, 1993; Jaffe *et al.* 1995). With one exception (Murphy *et al.* 1994), these studies have been conducted in the brain slice preparation. While the study of the spine in a slice provides important information on the dendritic spine in its natural environment, the depth of the dendritic spine in the tissue necessitates the use of low power, long-working distance objectives. Thus, the optical resolution obtained in the present study, with a ×100 1·3 NA objective is equal to or better than reported elsewhere. This is due to the two-dimensionality of the cultured neurons, but also to the fact that the dendritic spines on cultured neurons are not as dense as they are in the neuron *in situ*, allowing their study in relative isolation. Undoubtedly, the use of both the cultured neurons and those in the slice will advance our understanding of the role of the spine in neuronal integration.

The present results suggest that the spine and the adjacent dendrite are independent but closely associated calcium compartments; while there is a difference in the concentrations of calcium achieved during a response in the two compartments, the spine is likely to play an important role in boosting the rise in dendritic $[Ca^{2+}]_i$, such that a dendritic segment may behave differently from an adjacent segment with respect to their reactivity to afferent stimulation, and to their local rise of $[Ca^{2+}]_i$. The role of the individual spine in this larger functional unit has been alluded to in previous models (Segev & Rall, 1988) and will be subject to further studies.

ALFORD, S., FRENGUELLI, B. G., SCHOFIELD, J. G. & COLLINGRIDGE, G. L. (1993). Characterization of Ca^{2+} signals induced in hippocampal CA1 neurones by the synaptic activation of NMDA receptors. *Journal of Physiology* **469**, 693–716.

AOSAKI, T. & KASAI, H. (1989). Characterization of two kinds of high voltage-activated Ca channel currents in chick sensory neurons. *Pflügers Archiv* **414**, 150–156.

BENKE, T. A., JONES, O. T., COLLINGRIDGE, G. L. & ANGELIDES, K. J. (1993). N-Methyl D-aspartate receptors are clustered and immobilized on dendrites of living cortical neurons. *Proceedings of the National Academy of Sciences of the USA* **90**, 7819–7823.

BLISS, T. V. P. & COLLINGRIDGE, G. L. (1993). A synaptic model of memory: long term potentiation in the hippocampus. *Nature* **361**, 31–39.

CHANG, F. L. & GREENOUGH, W. T. (1984). Transient and enduring morphological correlates of synaptic activity and efficacy change in the rat hippocampal slice. *Brain Research* **309**, 35–46.

COLLINGRIDGE, G. L. (1992). The mechanism of induction of NMDA receptor-dependent long term potentiation in the hippocampus. *Experimental Physiology* **77**, 771–797.

CRAIG, A. M., BLACKSTONE, C. D., HUGANIR, R. L. & BANKER, G. (1993). The distribution of glutamate receptors in cultured rat hippocampal neurons: Postsynaptic clustering of AMPA-selective subunits. *Neuron* **10**, 1055–1068.

FIFKOVA, E., MARKHAM, J. A. & DELAY, R. J. (1983). Calcium in the spine apparatus of dendritic spines in the dentate molecular layer. *Brain Research* **266**, 163–168.

GLAUM, S. R., SCHOLZ, W. K. & MILLER, R. J. (1990). Acute and long term glutamate mediated regulation of $[Ca]_i$ in rat hippocampal pyramidal neurons in-vitro. *Journal of Pharmacology and Experimental Therapeutics* **253**, 1293–1302.

GRASSO, A., ALEMA, S., RUFFINI, S. & SENNI, M. I. (1980). Black widow spider toxin-induced calcium fluxes and transmitter release in neurosecretory cell line. *Nature* **283**, 714–716.

GRYNKIEWICZ, J., POENIE, M. & TSIEN, R. Y. (1985). A new generation of Ca indicators with greatly improved fluorescence properties. *Journal of Biological Chemistry* **260**, 3440–3450.

GUTHRIE, P. B., SEGAL, M. & KATER, S. B. (1991). Independent regulation of calcium revealed by imaging dendritic spines. *Nature* **354**, 76–80.

HELL, J. W., WESTENBROEK, R. E., WARNER, C., AHLIJANIAN, M. K., PRYSTAY, W., GILBERT, M. M., SNUTCH, T. P. & CATTERALL, W. A. (1993). Identification and differetial subcellular localization of the neuronal class C and class D L-type calcium channel $\alpha 1$ subunits. *Journal of Cell Biology* **123**, 949–962.

JAFFE, D. B., FISHER, S. A. & BROWN, T. H. (1994). Confocal laser scanning microscopy reveals voltage-gated calcium signals within hippocampal dendritic spines. *Journal of Neurobiology* **25**, 220–233.

KOCH, C. & POGGIO, T. (1983). A theoretical analysis of electrical properties of spines. *Proceedings of the Royal Society* B **218**, 455–477.

KOCH, C. & ZADOR, A. (1993). The function of dendritic spines: Devices subserving biochemical rather than electrical compartmentalization. *Journal of Neuroscience* **13**, 413–422

LEE, K. S., SCHOTTLER, F., OLIVER, M. & LYNCH, G. (1980). Brief bursts of high-frequency stimulation produce two types of structural change in rat hippocampus. *Journal of Neurophysiology* **44**, 247–258.

LYNCH, G., LARSON, J., KELSO, S., BARRIONUEVO, G. & SCHOTTLER, F. (1983). Intracellular injection of EGTA blocks induction of hippocampal long term potentiation. *Nature* **305**, 719–721.

MACDERMOTT, A., MAYER, M. L., WESTBROOK, G. L., SMITH, S. J. & BARKER, J. L. (1986). NMDA-receptor activation increases cytoplasmic calcium concentration in cultured spinal cord neurons. *Nature* **321**, 519–522.

MALENKA, R. C., KAUER, J. A., PERKEL, D. J. & NICOLL, R. A. (1989). The impact of postsynaptic calcium on synaptic transmission; its role in long term potentiation. *Trends in Neurosciences* **12**, 444–450.

MALINOW, R., OTMAKHOV, N., BLUM, K. I. & LISMAN, J. (1994). Visualizing hippocampal synaptic function by optical detection of Ca^{2+} entry through the N-methyl-D-aspartate channel. *Proceedings of the National Academy of Sciences of the USA* **91**, 8170–8174.

MARKRAM, H. & SAKMANN, B. (1994). Calcium transients in dendrites of neocortical neurons evoked by single subthreshold excitatory postsynaptic potentials via low-voltage-activated calcium channels. *Proceedings of the National Academy of Sciences of the USA* **91**, 5207–5211.

MINTZ, I. M., ADAMS, M. E. & BEAN, B. P. (1992). P-type calcium channels in rat central and peripheral neurons. *Neuron* **9**, 85–95.

MIYAKAWA, H., ROSS, W. N., JAFFE, D., CALLAWAY, J. C., LASSER-ROSS, N., LISMAN, J. & JOHNSTON, D. (1992). Synaptically activated increases in Ca^{2+} concentration in hippocampal CA1 pyramidal cells are primarily due to voltage-gated calcium channels. *Nature* **9**, 1163–1173.

MULLER, M., GÄHWILER, B. H., RIETSCHIN, L. & THOMPSON, S. M. (1993). Reversible loss of dendritic spines and altered excitability after chronic epilepsy in hippocampal slice cultures. *Proceedings of the National Academy of Sciences of the USA* **90**, 257–261.

MULLER, W. & CONNOR, J. A. (1991). Dendritic spines as individual neuronal compartments for synaptic Ca^{2+} responses. *Nature* **354**, 73–75.

MURPHY, T. H., BARABAN, J. M., WIER, W. G. & BLATTER, L. A. (1994). Visualization of quantal synaptic transmission by dendritic calcium imaging. *Science* **263**, 529–532.

PAPA, M., BUNDMAN, M. C., GREENBERGER, V. & SEGAL, M. (1995). Morphological analysis of the development of dendritic spines in primary cultures of hippocampal neurons. *Journal of Neuroscience* **15**, 1–11.

POZZO MILLER, L. D., PETROZZINO, J. J., MAHANTY, N. K. & CONNOR, J. A. (1993). Optical imaging of cytosolic calcium, electrophysiology and ultrastructure in pyramidal neurons of organotypic slice cultures from rat hippocampus. *Neuroimage* **1**, 109–120.

RALL, W. (1974). Dendritic spines, synaptic potency and neuronal plasticity. In *Cellular Mechanisms Subserving Changes in Neuronal Activity. Brain Information Service Report* No. 3, ed. WOODY, C. D., BROWN, K. A., CROW, T. J. & KNISPEL, J. D., pp. 13–21. University of California Press, Los Angeles.

REGEHR, W. G. & TANK, D. W. (1992). Calcium concentration dynamics produced by synaptic activation of CA1 hippocampal pyramidal cells. *Journal of Neuroscience* **12**, 4202–4223.

SEGAL, M. & GREENBERGER, V. (1992). Acidic amino acids evoke a smaller $[Ca]_i$ rise in GABAergic than non-GABAergic hippocampal neurons. *Neuroscience Letters* **140**, 243–246.

SEGAL, M. & MANOR, D. (1992). Confocal microscopic imaging of $[Ca^{2+}]_i$ in cultured rat hippocampal neurons following exposure to *N*-methyl-D-aspartate. *Journal of Physiology* **448**, 655–676.

SEGEV, I. & RALL, W. (1988). Computational study of an excitable dendritic spine. *Journal of Neurophysiology* **60**, 499–523.

TURNER, D. A. (1984). Conductance transients onto dendritic spines in a segmental cable model of hippocampal neurons. *Biophysical Journal* **46**, 85–96.

WADMAN, W. J. & CONNOR, J. A. (1992). Persisting modification of dendritic calcium influx by excitatory amino acid stimulation in isolated CA1 neurons. *Neuroscience* **48**, 293–305.

WICKENS, J. (1988). Electrically coupled but chemically isolated synapses: dendritic spines and calcium in a rule for synaptic modification. *Progress in Neurobiology* **31**, 507–528.

ZADOR, T., KOCH, C. & BROWN, T. (1990). Biophysical model of a Hebbian synapse. *Proceedings of the National Academy of Sciences of the USA* **87**, 6718–7622.

Acknowledgements

I wish to acknowledge Ms V. Greenberger for the preparation of the cultures, Dr S. B. Kater for help with the initial calcium measurements, and Dr M. Bundman for comments on earlier versions of the manuscript. This research was supported by The Basic Research Foundation administered by the Israel Academy of Sciences and Humanities, and by the Minerva Foundation, Munich, Germany.

Received 6 June 1994; accepted 18 January 1995.